

# Broadband single-mode operation of standard optical fibers by using a sub-wavelength optical wire filter

Yongmin Jung,\* Gilberto Brambilla, and David J. Richardson

*Optoelectronics Research Centre, University of Southampton, Southampton, SO17 1BJ, UK*

\*Corresponding author: [ymj@orc.soton.ac.uk](mailto:ymj@orc.soton.ac.uk)

**Abstract:** We report the use of a sub-wavelength optical wire (SOW) with a specifically designed transition region as an efficient tool to filter higher-order modes in multimode waveguides. Higher-order modes are effectively suppressed by controlling the transition taper profile and the diameter of the sub-wavelength optical wire. As a practical example, single-mode operation of a standard telecom optical fiber over a broad spectral window (400~1700 nm) was demonstrated with a 1 $\mu$ m SOW. The ability to obtain robust and stable single-mode operation over a very broad range of wavelengths offers new possibilities for mode control within fiber devices and is relevant to a range of application sectors including high performance fiber lasers, sensors, photolithography, and optical coherence tomography systems.

©2008 Optical Society of America

**OCIS codes:** (230.1150) All-optical devices; (060.2340) Fiber optics components; (220.4000) Microstructure fabrication; (220.4241) Nanostructure fabrication.

---

## References and links

1. K. Okamoto, *Fundamentals of Optical Waveguides* (Elsevier Academic, London, 2006).
2. J. Nilson, W. A. Clarkson, R. Selvas, J. K. Sahu, P. W. Turner, S. -U. Alam, and A. B. Grudinin, "High-power wavelength-tunable cladding-pumped rare-earth-doped silica fiber lasers," *Opt. Fiber Technol.* **10**, 5-30 (2004).
3. O. S. Wolfbeis, "Fiber-optic chemical sensors and biosensors," *Anal. Chem.* **74**, 2663-2678 (2002).
4. B. A. Flusberg, E. D. Cocker, W. Piyawattanametha, J. C. Jung, E. L. M. Cheung, and M. J. Schnitzer, "Fiber-optic fluorescence imaging," *Nature Methods* **2**, 941-950 (2005).
5. T. A. Birks, J. C. Knight, and P. St. J. Russell, "Endlessly single-mode photonic crystal fiber," *Opt. Lett.* **22**, 961-963 (1997).
6. P. St. J. Russell, "Photonic crystal fibers," *Science* **299**, 358-362 (2003).
7. L. Tong, R. R. Gattass, J. B. Ashcom, S. He, J. Lou, M. Shen, I. Maxwell, and E. Mazur, "Subwavelength-diameter silica wires for low-loss optical wave guiding," *Nature* **426**, 816-819 (2003).
8. G. Brambilla, V. Finazzi, and D. J. Richardson, "Ultra-low-loss optical fiber nanotapers," *Opt. Express* **12**, 2258-2263 (2004), <http://www.opticsinfobase.org/abstract.cfm?URI=oe-12-10-2258>.
9. S. Moon and D. Y. Kim, "Effective single-mode transmission at wavelengths shorter than the cutoff wavelength of an optical fiber," *IEEE Photon. Technol. Lett.* **17**, 2604-2606 (2005).
10. Denis Donlagic, "In-line higher order mode filters based on long highly uniform fiber tapers," *J. Lightwave Technol.* **24**, 3532-3539 (2006).
11. M. Sumetsky, Y. Dulashko, and A. Hale, "Fabrication and study of bent and coiled free silica nanowires: Self-coupling microloop optical interferometer," *Opt. Express* **12**, 3521-3531 (2004), <http://www.opticsinfobase.org/abstract.cfm?URI=oe-12-15-3521>.
12. D. -I. Yeom, E. C. Mägi, M. R. E. Lamont, M. A. F. Roelens, L. Fu, and B. J. Eggleton, "Low-threshold supercontinuum generation in highly nonlinear chalcogenide nanowires," *Opt. Lett.* **33**, 660-662 (2008), <http://www.opticsinfobase.org/abstract.cfm?URI=ol-33-7-660>
13. F. Xu, P. Horak, and G. Brambilla, "Optical microfiber coil resonator refractometric sensor," *Opt. Express* **15**, 7888-7893 (2007), <http://www.opticsinfobase.org/abstract.cfm?URI=oe-15-12-7888>.
14. V. I. Balykin, K. Hakuta, F. Le Kien, J. Q. Liang, and M. Morinaga, "Atom trapping and guiding with a subwavelength-diameter optical fiber," *Phys. Rev.* **A70**, 011401 (2004).
15. L. Tong, J. Lou, and E. Mazur, "Single-mode guiding properties of subwavelength-diameter silica and silicon wire waveguides," *Opt. Express* **12**, 1025-1035 (2004).

16. M. Sumetsky, Y. Dulashko, P. Domachuk, and B. J. Eggleton, "Thinnest optical waveguide: experimental test," *Opt. Lett.* **32**, 754-756 (2007).
  17. F. Bilodeau, K. O. Hill, S. Faucher, and D. C. Johnson, "Low-loss highly overcoupled fused couplers: Fabrication and sensitivity to external pressure," *J. Lightwave Technol.* **6**, 1476-1482 (1988).
  18. T. A. Birks and Y. W. Li, "The shape of fiber tapers," *J. Lightwave Technol.* **10**, 432-438 (1992).
  19. J. D. Love, W. M. Henry, W. J. Stewart, R. J. Black, S. Lacroix, and F. Gonthier, "Tapered single-mode fibres and devices - Part 1: Adiabaticity criteria," *IEE Proceedings-J* **138**, 343-354 (1991).
  20. R. J. Black, S. Lacroix, F. Gonthier, and J. D. Love, "Tapered single-mode fibres and devices - Part 2: Experimental and theoretical quantification," *IEE Proceedings-J* **138**, 355-364 (1991).
- 

## 1. Introduction

Stable single-mode operation in photonic waveguides [1] is a fundamental requirement within many areas of modern science and technology. The phenomenal growth in area such as high performance fiber lasers, sensors, photolithography, and optical coherent tomography systems [2-4] has increased the demand for short wavelength and wide-range single-mode operation. However, finding a means to achieve stable, low-loss and large mode area single-mode beam operation at short wavelengths and over a wide range of wavelengths represents a major technological challenge. Photonic crystal fibers [5,6] have been shown to exhibit endlessly single-mode operation but they present several issues including difficulty of fabrication, bend loss, air-hole contamination and challenge of reliably splicing such structures to conventional optical fibers. Here we show that sub-wavelength optical wires (SOWs) [7,8] can be used as an efficient means to provide higher-order mode filtering in multimode waveguides, allowing effective single mode operation of conventional optical fibers over an extended wavelength range. Compared to the previous taper-based higher-order mode filtering architecture [9,10], the proposed SOW opens up the prospect of the manipulation of photons in fibers in the sub-wavelength domain. Due to this sub-wavelength guidance, SOWs can tightly confine the optical beam to a small area and can be used to ensure the propagating light experiences a strong interaction with the surrounding medium, especially near the surface at the nano-scale. This technology has been proved advantageous to a wide range of applications such as high-sensitivity optical sensors, nonlinear optics, atom trapping and micro/nano-scale photonic devices [11-14]. In this study, we demonstrate how a sub-wavelength optical wire with specifically designed transition region can act as an efficient tool for higher-order mode filtering in multimode waveguides. A conventional telecom fiber with a 1  $\mu\text{m}$  SOW shows effectively endlessly single-mode operation with minimal optical loss ( $< 0.1\text{dB}$ ) for the fundamental mode.

## 2. Idealized sub-wavelength optical wire for higher-order mode filtering

### 2.1. Working principle, fabrication and optical transmission properties

Figure 1 represents an idealized SOW for higher-order mode filtering, which is composed of two conical transition tapers and a central uniform waist region. If the conical transition tapers are adiabatic, guided modes in the core of the multimode fiber ( $LP_{01}$ ,  $LP_{11}$  in Fig. 1(a)) are continuously mode converted to guided cladding modes in the SOW on a one-to-one basis by the down-taper and are then coupled back into guided modes in the multimode fiber by the up-taper. The evolution of the spatial profile of the first two guided modes along the transition tapers is also shown. However, higher-order modes can be effectively suppressed by controlling the SOW diameter in the uniform waist region [15], which serves to restrict the propagation of the higher-order modes along the entire length of the SOW and thereby constrains the number of guided modes at the taper output. In general, when the diameter of the optical fiber is considerably smaller than the wavelength of the guided light, the optical fiber can operate as a single-mode sub-wavelength-diameter waveguide with an air cladding. The single mode operation range is determined by the mode cut-off conditions commonly

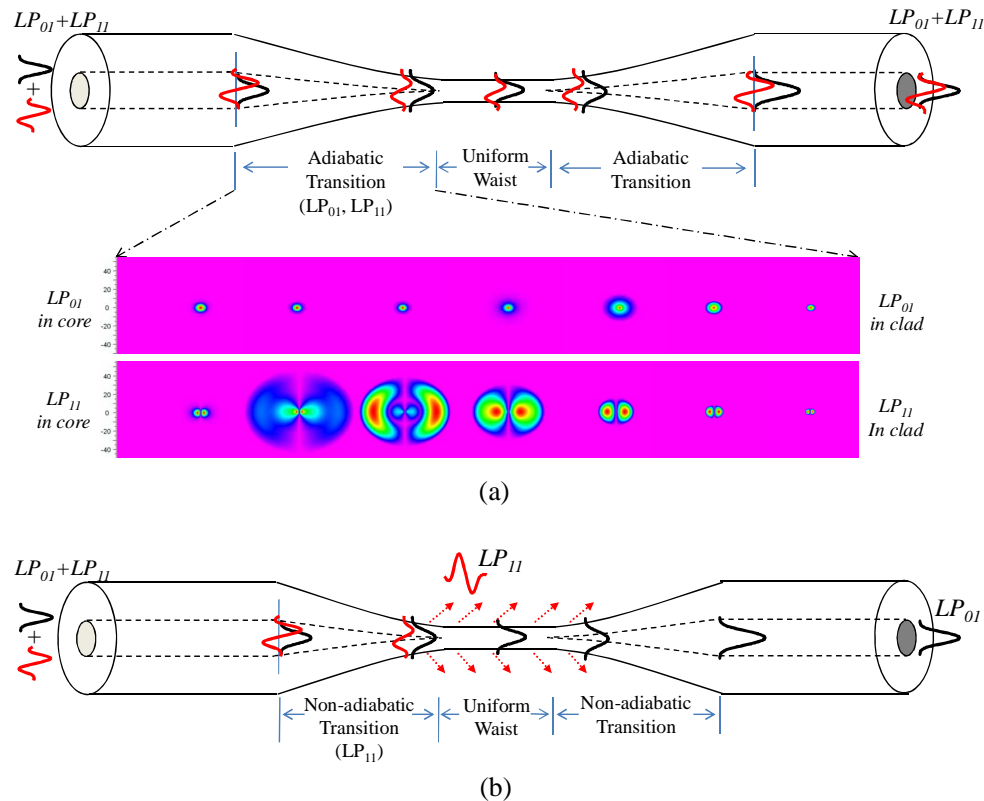


Fig. 1. An idealized sub-wavelength optical wire (SOW) for higher-order mode filtering in a two mode optical fiber. (a) Adiabatic transition tapers provide continuous mode evolution from core modes to cladding modes, and *vice versa*. All modes launched into the fiber are collected at the fiber output. (b) The use of non-adiabatic tapers for higher-order core modes transfers power to higher-order cladding modes or radiation modes which are not guided by the SOW. Higher-order taper modes are effectively filtered out by controlling the SOW diameter.

used for larger waveguides [1,15,16] and single-mode operation is limited to a spectral range of just a few hundred nanometers; at short wavelengths the SOW still supports a finite number of high-order modes. By designing an appropriate non-adiabatic transition taper as shown in Fig. 1(b), it is possible to convert high-order core modes to higher-order cladding modes or radiation modes which are not supported by the SOW. The different mode evolution (adiabatic for fundamental mode and non-adiabatic for higher-order modes) allows only the transverse single mode to propagate along the waveguide, which permits single-mode operation for a conventional fiber over an extremely wide range of wavelengths. Low-loss SOWs were manufactured with the aid of the well-established single-stage conventional “flame-brushing” technique [17]. A standard telecom optical fiber (Corning SMF-28) was selected as a simple example of a fiber providing multimode operation at short wavelengths. The profile of the conical transition tapers in the experiment was approximated by a decreasing exponential function (transition region length  $\sim 25$ mm, uniform waist length  $\sim 4$ mm, relative taper elongation rate=0 [18]) and was achieved by ensuring appropriate control of the translation stage movement during the tapering process [8,18].

To investigate the modal guidance, *in-situ* transmission spectra of the SOWs were recorded for various outer diameters during the fabrication. Figure 2(a) shows the spectral output of a telecom optical fiber for different diameters in the uniform waist region. Two spectral regions can be observed in the untapered fiber ( $125\mu\text{m}$ ): above  $1250\text{nm}$  the fiber behaves as a single-mode waveguide, while below  $1250\text{nm}$  two or more modes are supported:

this is clearly seen by the increased fiber output in the range 850~1250 (where two modes are supported) with respect to the single-mode operation range above 1250nm. Figure 2(a) shows that, as the waist diameter is decreased from 125 to 70 $\mu\text{m}$ , intermodal interference appears in the multimode spectral region, while no perturbation occurs in the single-mode operation range. This can be explained by a conical transition region that is adiabatic for the fundamental mode but non-adiabatic for higher-order core modes, which results in the excitation of higher-order cladding modes which interfere and beat. When the outer diameter reaches 4 $\mu\text{m}$  the higher-order mode cut-off shifts to shorter wavelengths, enlarging the single-mode operation region. Note that for the 1 $\mu\text{m}$  SOW there is no higher-order mode cut-off and the optical loss is negligible ( $< 0.1\text{dB}$  at  $\lambda=1.55\mu\text{m}$ ). Moreover, bending losses come into effect at long wavelengths in SOWs with a diameter of less than 700nm due to their weak guidance. Therefore, it appears that the optimum SOW diameter for efficient higher-order filtering is about 1 $\mu\text{m}$ . Generally, the single-mode operation bandwidth is limited at short wavelengths by a higher-order mode cut-off ( $\lambda_{c\_LP_{11}}$ ,  $\lambda_{c\_LP_{21}}$  and  $\lambda_{c\_LP_{02}}$  in standard optical fibers) as shown in Fig. 2(b). However, by applying the efficient mode filtering scheme based on a sub-wavelength waveguide, a very broad range of single-mode operation (400~1700nm) was successfully realized with minimal loss (red line in Fig. 2(b)).

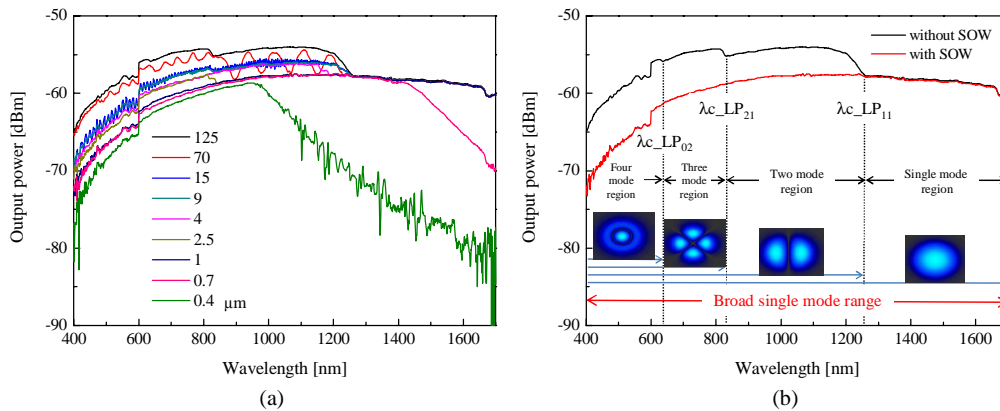


Fig. 2. Spectral response of the tapered fibers: (a) Transmission spectra of a 5m telecom fiber with a SOW for different SOW outer diameters. Interference between different modes occurs for tapers with 70 $\mu\text{m}$  diameter, while single mode operation is observed for the whole range of scanned wavelengths for tapers with 1 $\mu\text{m}$  diameter. (b) Comparison between the transmission spectra of a standard fiber (Corning SMF-28) without (in black) and with (in red) a 1 $\mu\text{m}$  SOW.  $\lambda_{c\_LP_{11}}$  represents the cut-off wavelength for the bi-lobed  $LP_{11}$  mode which exists only for wavelengths shorter than  $\lambda_{c\_LP_{11}}$ . Similarly,  $\lambda_{c\_LP_{21}}$  and  $\lambda_{c\_LP_{02}}$  represent the cut-offs for the higher order modes  $LP_{21}$  and  $LP_{02}$ , respectively.

## 2.2. Stability of single-mode operation

To confirm robust single-mode guidance, the far-field pattern was imaged with a 50 $\times$  microscopic lens and a CCD camera captured the image at the wavelength of 635 (He-Ne laser, KD Optics) and 488nm (Ar<sup>+</sup> laser, Omnicrome). Generally, when coherent light is guided within a multimode fiber, interference between guided modes travelling within the fiber results in the degradation of the laser beam quality at the waveguide output. In fact, the interference pattern is extremely sensitive to external perturbations such as bending. As predicted, the conventional fiber (i.e. without the SOW mode filter) suffers severe modal interference when bending is applied as shown in Figs. 3(left: a,c,e). However, when a SOW is inserted, the fiber output showed a high-quality single-mode beam which was not disturbed by external bends (Figs. 3(right: b,d,f)). Note that clear single mode characteristics were obtained at the edge of the claimed spectral range of single-mode operation. To test the stability of the single mode operation external perturbations such as bends and multi-point

splices were applied to the SMF beyond the SOW filter: no form of optical degradation was detected in the mode profile and/or in the transmission spectrum.

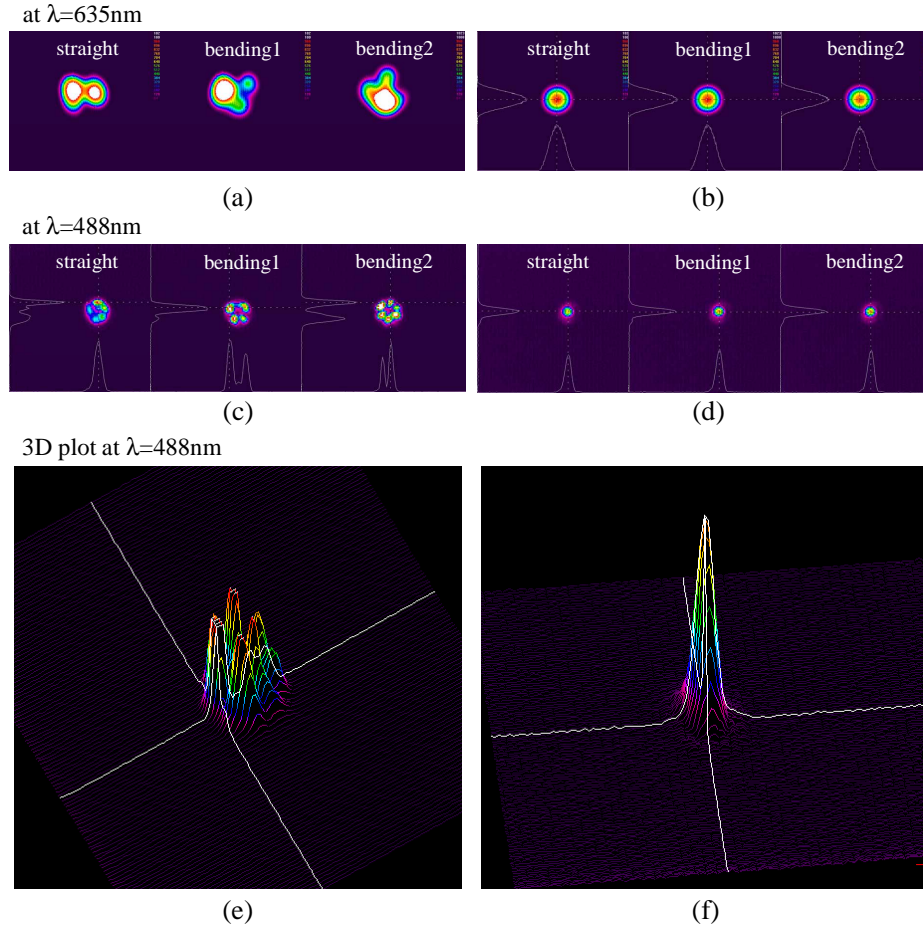


Fig. 3. Far-field imaging of telecom fibers without (a,c,e) and with SOW (b,d,f) at a wavelength of 632.8nm (He-Ne laser) and 488 nm (Ar laser), respectively.

### 3. Analytic modeling of mode evolution

To allow a more detailed understanding of the optical mode evolution along the transition taper, the adiabaticity of the transition taper has been examined by calculating the beat length and taper angle necessary to ensure adiabatic behavior [19,20]. A profile is called adiabatic for a mode when it does not induce any power transfer to any other mode. Figure 4(a) and (b) plot the calculated effective indices of the guided modes as a function of the core guidance parameter ( $V$ -value) for an input wavelength  $\lambda=1\mu\text{m}$ . In an ideal adiabatic transition taper, the taper angle is small enough so that the  $LP_{01}$ ,  $LP_{11}$  core modes can be considered unperturbed as they evolve from being core-guided to cladding-guided. In particular, the beat length  $z$  between two modes having propagation constants  $\beta_1$  and  $\beta_2$  in a fiber with radius  $\rho$  has been assumed to be the defining factor determining the transition between lossless and lossy tapers. For distances larger than the beating length the two modes do not exchange power and the taper is adiabatic. This results in the critical angle  $\Omega$  being defined as:

$$\Omega = \frac{\rho}{z} = \frac{\rho(\beta_1 - \beta_2)}{2\pi} \quad (1)$$

Within non-adiabatic conditions, the core mode couples to higher-order cladding modes of the same symmetry [18]. The coupling to the next high order mode ( $LP_{0l} \rightarrow LP_{02}$ ,  $LP_{1l} \rightarrow LP_{12}$ ,  $LP_{2l} \rightarrow LP_{22}$ ) is dominant with respect to the coupling to other higher order modes ( $LP_{0l} \rightarrow LP_{03}$ ,  $LP_{1l} \rightarrow LP_{13}$ ,  $LP_{2l} \rightarrow LP_{23}$ ) and it represents the limiting factor for an adiabatic transition at a particular physical taper radius. As an example the adiabatic transition angle  $\Omega$  for  $LP_{0l}$  and  $LP_{1l}$  modes has been evaluated at  $\lambda=1\mu\text{m}$  by applying equation (1) to the curves in Figs. 4(a) and (b). There are significant differences in the adiabatic criteria of the fundamental and high-order modes, as shown in Fig. 4(c): the delineating curve of the  $LP_{1l}$  mode transition is located at small tapering angles, meaning that the  $LP_{1l}$  mode needs an extremely well-controlled small taper angle and a relatively longer taper transition length. The exponential taper profile used in this set of experiments had a transition region of about 25mm and is shown in blue in Fig. 4(c). The exponential taper lies in the lossy region of the adiabatic taper curve for the  $LP_{1l}$  mode for inverse tapering ratios between 0.65 and 0.8. This simulation results

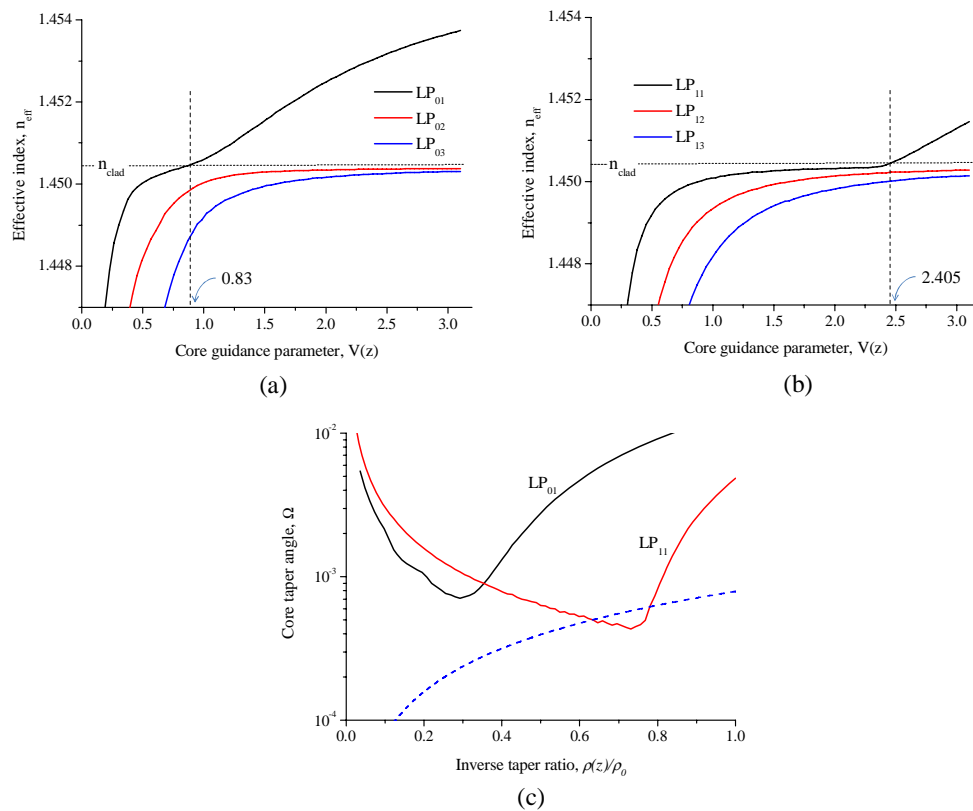


Fig. 4. Effective index versus core guidance parameter  $V (=2\pi\rho NA/\lambda$ , where  $\rho$  is the SOW radius,  $NA$  the numerical aperture and  $\lambda$  the wavelength) for the first three (a)  $LP_{0m}$  and (b)  $LP_{1m}$  guided modes.  $n_{\text{clad}}$  and  $n_{\text{eff}}$  represent the cladding and the mode effective indices, respectively. The difference of effective indices between  $LP_{n0}$  and  $LP_{n1}$  modes allows the determination of the taper adiabatic angle  $\Omega$  through equation 1. (c) Adiabatic profiles for  $LP_{0l}$  (black) and  $LP_{1l}$  (red) modes. The real taper profile has greater angles than the  $LP_{1l}$  adiabatic curve between inverse taper ratios  $\rho(z)/\rho_0=0.65$  and  $0.8$ , meaning that the  $LP_{1l}$  mode will be converted in  $LP_{1m}$  ( $m>1$ ) modes for  $\rho(z)/\rho_0<0.8$ .

provide good agreement with the measured spectral response in Fig. 2, for which it predicts non-adiabatic propagation for the  $LP_{11}$  mode for diameters smaller than  $100\mu\text{m}$ ; the excitation of other higher-order cladding modes results in oscillations in the higher-order mode spectral region (below  $1250\text{nm}$ ) and a significant excess loss. Another important feature of the modal calculation is that it can be used to design a more optimal adiabatic taper shape. The delineating curve for  $LP_{01}$  should provide a solution for optimal taper shape (less than few mm). This aspect has been pursued further by the authors and will be reported elsewhere in due course.

#### **4. Conclusions**

In conclusion, a compact simple scheme for stable single-mode operation of multimode waveguides has been developed and validated. Different mode evolutions (adiabatic for fundamental mode and non-adiabatic for higher-order modes) along sub-wavelength-sized waveguides produce significantly different losses. Higher-order modes are effectively suppressed by controlling the transition taper profile and the diameter of the sub-wavelength optical wire. While the transition taper transfers power from the second and third order modes to unguided and higher order modes, the small diameter SOW brings further suppression by constraining the number of guided cladding modes. As an example, single-mode operation of a standard telecom optical fiber over a broad spectral window ( $400\sim 1700\text{nm}$ ) was demonstrated with a  $1\mu\text{m}$  SOW. The stable single-mode operation could be very beneficial for various applications in fiber lasers, sensors, photolithography, and optical coherence tomography.

#### **Acknowledgments**

The authors thank the Engineering and Physical Sciences Research Council UK for financial support; GB gratefully acknowledges the Royal Society (UK) for his Research Fellowship.